International Journal of Thin Film Science and Technology

Volume 10
Issue 2 *May 2021*

Article 2

2021

Features of n-SnO2 / p-Si Structural Heterojunction Manufactured by the Chemical Steam-Gas Deposition Method

Mardonbek Ulugbekovich Hajiev
Physical Technical Institute, Uzbekistan Academy of Sciences, 100084 Tashkent, Uzbekistan,
philominathan@gmail.com

Rustam Rashidovich Kabulov
Physical Technical Institute, Uzbekistan Academy of Sciences, 100084 Tashkent, Uzbekistan,
krr1982@bk.ru

International Journal of Thin Films Science and Technology

http://dx.doi.org/10.18576/ijtfst/100202

Features of *n*-SnO_2 / *p*-Si Structural Heterojunction Manufactured by the Chemical Steam-Gas Deposition Method

Mardonbek Ulugbekovich Hajiev[*] *and Rustam Rashidovich Kabulov*

Physical Technical Institute, Uzbekistan Academy of Sciences, 100084 Tashkent, Uzbekistan

Received: 21 Feb. 2020, Revised: 22 Mar. 2020, Accepted: 24 Mar. 2020.
Published online: 1 May 2021

Abstract: By the method of chemical vapor-gas deposition (CVD) SnO_2 layers have been grown at the temperature of 170-500°C on the surface of *p*-Si single crystals with the (111) direction; the wafers had a thickness of 500 μm. A special evaporator with a temperature of 80-120°C has been used to obtain saturated steam in a quasi-closed reactor. The grown n-SnO_2 layers had a microcrystalline structure. Based on the analysis of X-ray diffraction and the dark current – voltage characteristics, an energy-band diagram of the *n*-SnO_2/*p*-Si heterostructure is constructed.

Keywords: semiconductor, SnO_2, Si, Chemical vapor deposition, microcrystalline, heterostructure, X-ray diffraction, dark current – voltage characteristic, energy-band diagram.

1 Introduction

Tin oxide (SnO_2) is the semiconductors with a wide band gap (3.6 ~ 3.9 eV) and is one of the important materials for optoelectronic technology. Since SnO_2 layers are used in various fields of technology and instrumentation, research and improvement of their characteristics are still being carried out [1]. For the synthesized SnO_2 films used varies methods: magnetron sputtering, [2-6] pulsed laser deposition (PLD), [7-10] ultrasonic sputtering methods [11, 12], sol-gel method [13] and etc. [14].

Increasing growth rate of SnO_2 films, will getting to increase the layer thickness, also to decrease the series resistance, but increased the efficiency of solar cells based on SnO_2 films. This task has been performed in the framework of the modernized SGD (steam-gas deposition) method for growing polycrystalline SnO_2 films [15, 16].

The SGD method allows growing polycrystalline SnO_2 semiconductor films by the pyrolytic vapor decomposition of tin compounds at substrate temperatures of 170-500°C [15, 16]. Stream of carrier gas (Argon, Helium, etc.) is used to deliver reagent vapors to the front of crystallization. In this case, it is also necessary to control the partial pressure of oxygen in the reactor. The film growth rate is in the range of 0.5-1.0 μm/hour by this method. Since the temperature of the carrier gas is significantly lower than the temperature of the substrate, the vapor pressure of the reagents is less than the maximum possible upon receipt of sufficiently high-quality SnO_2 films. Only a small part of the molecules reaches the crystallization front, the rest of part is carried away by the carrier gas stream. The bulk of unreacted components and reaction products are deposited on other nodes of the growth equipment. This fact, which is not important in laboratory experiments, becomes important in the mass production of structures.

The conductivity of SnO_2 films at room temperature can be controlled both by doping with small donor and acceptor impurities, and by introducing structural defects with a low ionization energy of 30-140 meV (oxygen vacancies) [17]. A review of the properties of SnO_2 films obtained by various methods, including thermal sputtering in vacuum, magnetron sputtering of synthesized source targets, chemical vapor-gas epitaxy using indium and tin acetates, indium and tin chlorides, indium trimethines and other reagents used in SnO_2 growth, is given in [18].

In the usual spray pyrolysis method, drops of the reagent solution are supplied directly to the heated substrate, part of the reagents, thermally decomposing, interacting with oxygen, form oxide molecules on the surface of the substrate. The undecided portion of the reactants and reaction products are carried away by the carrier gas stream. In our case, SnO_2 - films were grown in a laboratory setup, in a quasi-closed volume (there is no

[*]Corresponding author E-mail: philominathan@gmail.com

carrier gas flow), using a separate evaporator with a temperature of 80-120°C, to create a saturated vapor-gas phase in the reactor. This made it possible, on the one hand, to reduce the consumption of reactants, and, on the other hand, to increase the growth rate by 5-10 times [16]. In Fig.1.a block diagram of the developed setup for producing SnO_2 films is presented.

In this work, an *n*-type polycrystalline semiconductor SnO_2 film was deposited by chemical vapor-gas deposition at a substrate temperature of 260°C on a polished *p*-type single crystal Si wafer. The vapor-gas phase is created by the evaporator (4) located in the lower part of the installation; the temperature of the evaporator is selected so that it does not exceed the decomposition temperature of tin chloride molecules.

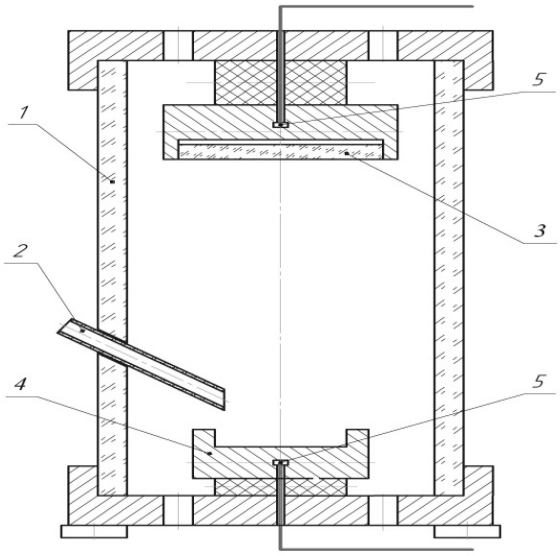

Fig.1: Block diagram of the setup for producing SnO_2 films on various substrates in the temperature range 170-500°C: 1 -quartz reactor; 2 -tube for supplying the reagent solution to the evaporator; 3 - substrate; 4 - evaporator; 5- thermocouples to control the temperature of the substrate and the evaporator [19]

The SnO_2 film served as a photo window for a Si-based photovoltaic device, and also as a semiconductor layer that forms space charge regions and built-in potentials in the heterojunction. Since the electron affinity energy of SnO_2 is approximately 4.5 eV and is lower than for *p*-Si [18]. The SnO_2 frontal layer also serves as an antireflection coating and as an electrical frontal collecting contact. The n-SnO_2/p-Si heterojunction photovoltaic device can convert sunlight into electrical energy through a two-layer - two-band structure: high-energy photons ($h\nu > E_g(SnO_2)$) will be absorbed in the SnO_2 layer, while low-energy photons $h\nu < E_g(SnO_2)$, the visible and infrared spectral regions will be absorbed in *p*-Si and converted into electrical energy. The not absorbed spectral regions of sunlight reflected and pass through the front SnO_2 layer.

2 Experimental Sections

2.1 Preparation of n-SnO_2/p-Si heterostructures

As mentioned above, for the *n*-SnO_2/*p*-Si heterostructure silicon with *p*-type conductivity (SDB-1) served as a substrate. The thickness of the wafer used was 500 μm with an (111) crystal orientation. The plate was pre-cleaned by immersion in a 15% HF solution for two minutes to remove the natural oxide layer.

Polycrystalline SnO_2 films were deposited on a polished single-crystal *p*-Si substrate using the developed technique (Fig. 1), in a quasi-closed volume. To spray the $SnCl_4$ solution a medical pipette was used. The solution used had a concentration of 0.2 M and consisted of a mixture of $SnCl_4 + 5H_2O$. A mixture of $SnCl_4 + 5H_2O$ was supplied from the tube (2) to the lower hot plate (4). $SnC1_4$ vapors are contained in a quasi closed volume, chemically interacting with oxygen contained in air, according to relation (1), form tin oxide SnO_2 [18].

$$SnCl_4 + O_2 \rightarrow SnO_2 + 2Cl_2 \qquad (1)$$

The substrate (3) on a holder was kept at the appropriate temperature.

The structure of the created *n*-SnO_2/*p*-Si heterojunction presented in Fig. 2. An InGa alloy with a thickness of 1 μm in the form of a grid was deposited on the surface of SnO_2 layer to create an upper collecting electrode.

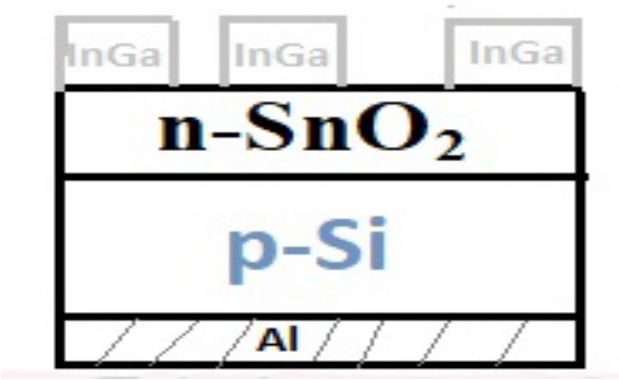

Fig.2: Design of *n*-SnO_2/*p*-Si structural heterojunction.

The aluminum contact served as the lower collecting electrode, which was 1 μm thick, was deposited on the back of the silicon substrate by vacuum thermal evaporation of Al. The photoactive area of the device was 1 cm^2.

The thickness of the SnO_2 films was measured using an interference microscope. The microstructure of the films was studied using a DRON-UM1 (CuKα) X-ray diffractometers. Absorption spectra were studied on a SPECTRUM BX II IR Fourier spectrometer (Perkin Elmer). Current-voltage (I-V) characteristics were studied on a complex for measuring the current-voltage characteristics of Oriel Sol3A class AAA.

Table 1 shows the main electrophysical parameters of the synthesized transparently conducting layers of SnO_2 films.

Table1: Electrophysical parameters of transparently conducting SnO_2 films.

	Band gap (eV)	Conductivity $(Ohm \cdot cm)^{-1}$	Electron concentration (cm^{-3})	Mobility $(cm^2V^{-1}s^{-1})$
SnO_2	3.6	5000	$>10^{20}$	15

3 Experimental Results

3.1 Assessment of Crystalline Phase

In Figure 3 shows the X-ray diffraction pattern of polycrystalline SnO_2 films grown, at the substrate temperature of 220°C, deposited on the surface of polished p-type silicon, investigated using a DRON-UM1 X-ray diffractometer (CuKα). The study showed that the obtained SnO_2 films have a polycrystalline phase. X-ray diffraction (XRD) peaks at 26.68°, 34.04°, 38.12°, 51.88° and 54.55° corresponded to the SnO_2 phase from the (110), (101), (200), (211) and (220) planes, respectively [18, 19]. The peak (XRD) from the plane (101) in amplitude was the strongest. This orientation corresponds to the tetragonal phase of SnO_2. Accordingly, upon the deposition of the SnO_2 film, a tetragonal rutile structure is formed. On the other hand, in the X-ray diffraction pattern of polycrystalline SnO_2 films grown at a substrate temperature of 220°C, no peaks associated with the tin monoxide phase SnO were detected.

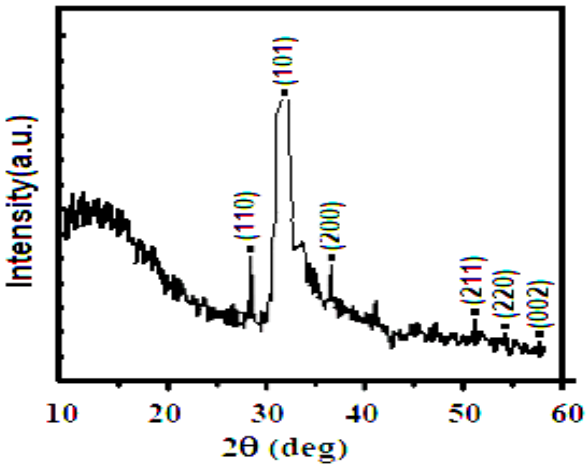

Fig. 3: Diffraction patterns of SnO_2 films grown at the substrate temperature of 220°C investigated using a DRON-UM1 X-ray diffractometer (CuKα).

3.2. Dark current-voltage characteristics

Dark current-voltage characteristics of the *n*-SnO_2/*p*-Si heterojunction are shown in Figure 4.

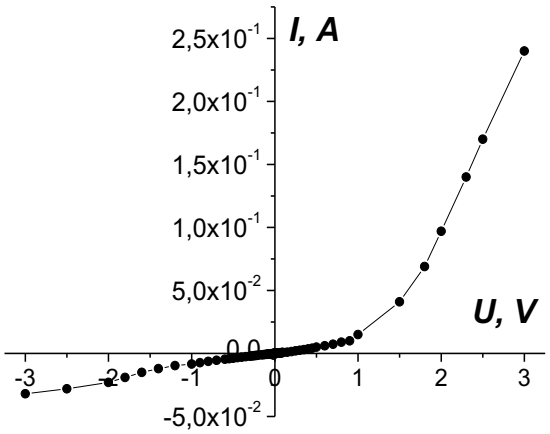

Fig.4: Dark current-voltage characteristic of a SnO_2/*p*-Si heterojunction based on a polycrystalline SnO_2 layer.

The current-voltage characteristic of the *n*-SnO_2/*p*-Si heterojunction (Fig. 4) shows the rectification coefficient (the ratio of the value of the magnitude of the forward current to the reverse current at a certain value of the electric voltage J_{for} / J_{rev}), with the applied voltage V = 3 Volts, is 10. In the figure 5 shows the dark I–V characteristic of the *n*-SnO_2/*p*-Si heterojunction constructed on a double logarithm scale. It can be seen from the above dependence that the I–V characteristic for both forward and reverse directions is described by relation (2):

$$J = A \cdot V^m \qquad (2)$$

The I–V characteristic in the reverse direction from 10^{-3} Volts to 1 Volt is determined by the linear dependence of current on voltage, that is, Ohm's law ($m \approx 1$) is satisfied [20]. From this section, we can determine the resistance of the base region of the *n*-SnO_2/*p*-Si heterojunction. In the case of a reverse current direction, it is ≈ 220 Ohm. In the region of bias voltage V> 1.1 V, an injection region is observed ($m \approx 2$) [21].

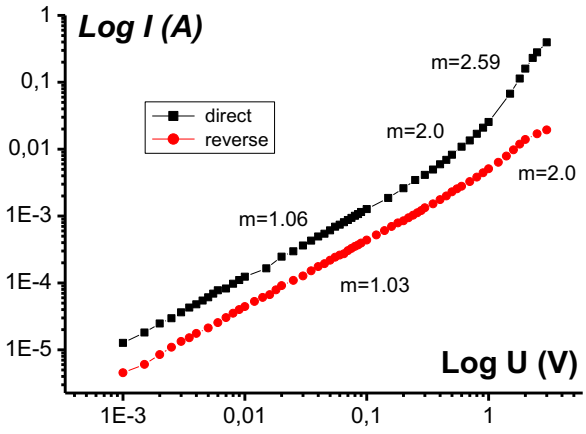

Fig. 5: Dark I–V characteristic of the *n*-SnO_2/*p*-Si photoelectric heterojunction constructed on a double logarithm scale

The I–V characteristic in the forward direction from 10^{-3} Volts to 0.2 Volts is determined by the linear dependence of the current on voltage, i.e., Ohm's law is fulfilled (m ≈1). From this section, it is possible to determine the resistance value of the quasineutral part of the n-SnO_2/p-Si heterojunction. In the case of the forward direction, it is ≈80 Ohm. In the region of bias voltage V> 0.3 Volts, an injection region is observed (m ≈ 2). In the region of the bias voltage V> 0.8 V, an injection region with a power exponent m ≈ 3 is observed. A change in the value of the exponent (m) from 2 to 3 is explained by the inclusion of recombination complexes in the generation – recombination process [22].

3.3. Energy band diagram

Energy band diagram of the *n*-SnO_2/*p*-Si structural heterojunction are shown in Figure 6.

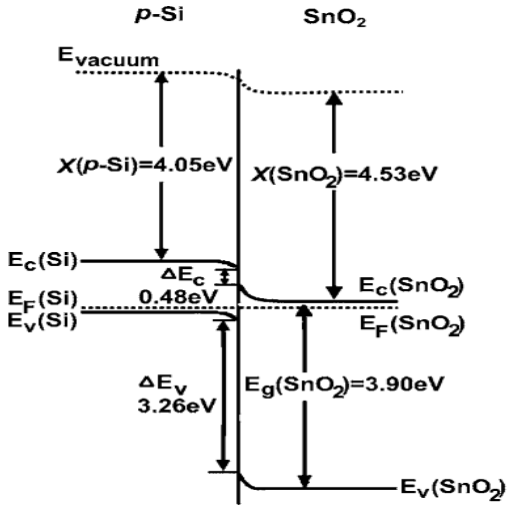

Fig. 6: Energy band diagram of the *n*-SnO_2/*p*-Si structural heterojunction [14].

The electron affinity of the semiconductor SnO_2 layer is χ_{SnO2} ≈ 4.53 eV [14] and it is lower than for *p*-Si χ_{Si} ≈ 4.05 eV, which leads to the formation of a depletion region by the main charge carriers at the interface of the n-SnO_2/p-Si layers and forms an integrated Barrier potential in the *n*-SnO_2/*p*-Si structure. At the boundary of the heterojunction in the conduction and valence bands, a gap ΔE_c and ΔE_v is formed due to the differ forbidden bands (E_{gSi}, E_{gSnO2}) of the contacting materials (*n*-SnO_2/*p*-Si).

The formation of the injection region in the reverse branch of the I–V characteristic of the *n*-SnO_2/*p*-Si structural heterojunction (Figure 5) is explained by the fact that there is a reverse biased barrier to the main barrier at the *p*-Si and Al interface, since the work function of Al (χ_{Al} ≈ 4.2 eV) [23] is less work function for *p*-Si (χ_{Si} + Eg_{Si} - E_{FpSi} ≈ 5.5 eV), as a result, the Al/*p*-Si Schottky barrier is formed. At external voltage when the drop on the Al/*p*-Si barrier becomes larger than on the *n*-SnO_2/*p*-Si barrier, electron injection will begin in the *p*-Si layer from the Al contact.

4 Conclusions

A thin transparent conductive film of tin oxide (SnO_2) was synthesized on the surface of a polished silicon wafer with *p*-type conductivity by pyrolytic vapor decomposition of tin chloride ($SnCl_4$) in a quasi-closed volume and a *n*-SnO_2/*p*-Si heterojunction device was fabricated. The deposition of the film was carried out at a substrate temperature of 220°C. The developed system for the deposition of transparently conducting layers of metal oxides in a quasiclosed volume is very cheap and convenient. SnO_2 films have a polycrystalline structure. The *n*-SnO_2/*p*-Si heterojunction device exhibits an obvious rectifying characteristic. *n*-SnO_2/*p*-Si structure can be used to register monochromatic radiation sources in the ultraviolet, visible, and near infrared regions.

Acknowledgement

The authors would like to thank Khimmatli Juraev, Usmonkhoja Sodikov and Abdurasul Gulyamov for assisting during the proofreading of the manuscript. This work was financially supported by the Program for Fundamental Research Grant number BA-FA-F-2-005.

References

[1] Xiangping Chen, Jianyu Liang, Zhentao Zhou, Huanan Duan, Boquan Li, Qiming Yang. The preparation of SnO_2 film by electrodeposition. *Mater. Res. Bull.* **45**, 2006-2011 (2010).

[2] R.Y. Korotkov, P. Ricou, A.J.E. Farran, Preferred orientations in polycrystalline SnO_2 films grown by atmospheric pressure chemical vapor deposition. *Thin Solid Films* **502**, 79 (2006).

[3] M. Ruske, G. Bräuer, J. Pistner, U. Pfäfflin, J. Szczyrbowski. Properties of SnO_2 films prepared by DC and MF reactive sputtering. *Thin Solid Films* **351**, 146-150 (1999).

[4] Dan Leng, Lili Wu, Hongchao Jiang, et al., Preparation and Properties of SnO_2 Film Deposited by Magnetron Sputtering. *International Journal of Photoenergy* **235,** 971, (2012).

[5] Tailong Gui, Long Hao, Jianmin Wang, et al. Structure and features of SnO_2 thin films prepared by RF reactive sputtering *Chinese optics letters* **8**, 1671, (2010)

[6] Sung Uk Lee, Won Seok Choi, Byungyou Hong, Synthesis and characterization of SnO_2:Sb film by dc magnetron sputtering method for applications to transparent electrodes. *Phys. Scr.* **T129**, 312 (2007).

[7] H. Cachet, J. Bruneaux, G. Folcher, n-Si/SnO_2 junctions based on macroporous silicon for photoconversion. *Solar Energy Materials and Solar Cells.* **46, (2),** 101-114 (1997)

[8] Z.W. Chen, J.K.L. Lai, C.H. Shek, Nucleation and growth of SnO_2 nanocrystallites prepared by pulsed laser deposition. *Appl. Phys. A* **81**, 959–962 (2005)

[9] E. Chan y Diaz, A. Duarte-Moller, Juan M. Camacho, SnO_2 thin films grown by pulsed Nd:YAG laser deposition. *Applied Physics A* **106**, 619–624 (2012)

[10] ZHAO Songqing, ZHOU Yueliang, WANG Shufang. Effect of ambient oxygen pressure on structural, optical and electrical properties of SnO_2 thin films. *RARE METALS* **25, (6),** 693-696 (2006)

[11] R.Chandrasekhar, K.L.Choy. Innovative and cost-effective synthesis of indium tin oxide films. *Thin Solid Films* **398**, 59-64 (2001)

[12] Y. Sawada, C. Kobayashi, S. Seki, H. Funakubo, Highly-conducting indium□tin-oxide transparent films fabricated by spray CVD using ethanol solution of indium (III) chloride and tin (II) chloride. *Thin Solid Films* **409, (1),** 46-50. (2002)

[13] Zhengtian Gu, Peihui Liang, Xiaolin Liu, Weiqing Zhang, Yueqin Le, Characteristics of Sol-Gel SnO_2 Films Treated by Ammonia. *J. Journal of Sol-Gel Science and Technology* **18,** 159–166 (2000).

[14] Zhizhong Yuan, Dongsheng Li, Minghua Wang, Peiliang Chen, Daoren Gong, Peihong Cheng, Deren Yang. Electroluminescence of SnO_2/p-Si heterojunction. *Appl. Phys. Lett.* **92,** 121-908 (2008)

[15] I. G. Atabaev, M. U. Hajiev, V. A. Pak, S. B. Zakirova, Kh. N. Juraev. Growth of transparent electrical conducting films of indium and tin oxides by chemical vapor deposition. *Applied Solar Energy* **52,** 118–121(2016)

[16] Atabaev I.G. Khajiev M.U., Pak V.A., Zakirova S.B. Method of growing ITO films by chemical vapor deposition. *Patent* UZ **IAP 05674** (2018)

[17] B. Kamp, R. Merkle, R. Lauck, J. Maier. Chemical diffusion of oxygen in tin dioxide: Effects of dopants and oxygen partial pressure. *Journal of Solid State Chemistry*. **178, (10),** 3027-3039 (2005)

[18] BO HE., Jing Xu, Huaizhong Xing, Chunrui Wang, Ying Guo And Hongwei Lu. Observation of nanospherical n-SnO_2/*p*-Si heterojunction fabricated by ultrasonic spray pyrolysis technique. *Surface Review and Letters* **20, (5),** 1350052 (2013)

[19] I.G. Atabaev, M.U. Hajiev and V.A. Pak. Growth of ITO Films by Modified Chemical Vapor Deposition Method. Int. *J. Thin. Fil. Sci. Tec.* **5**, **(1)**, 1-9 (2016)

[20] Kobulov R.R., Makhmudov M.A., Gerasimenko S.Y., Ataboev O.K. Morphology and Current transport in a thin-film polycrystalline Au-$Zn_xCd_{1-x}S$-Mo structure with a wide photosensitivity range in the ultraviolet and visible radiation spectral region. *Applied Solar Energy.* **54, (4),** 251-254 (2018)

[21] R. R. Kabulov, M. A. Makhmudov,O. K. Ataboev & M. U. Khazhiev. The study of factors that influence on the effectiveness of the photoconversion of n-CdS/*p*-CdTe heterostructures. *Applied Solar Energy*, **52**, **(1)**, 61-67 (2016)

[22] R.R.Kobulov, M.A.Makhmudov, S.Y.Gerasimenko, O.K.Ataboev. Investigation of composition and current transport mechanism in polycrystalline thin film ultra violet Au-$Zn_XCd_{1-X}S$-Mo- structure with narrow spectrum of photosensitivity. *App.Solar Energy,* **53 (2),** 123-125 (2017)

[23] Approx band offsets: Robertson JAP 2006 and *http://ematsolar.lbl.gov/images. CRC Workfns: http://www.hbcpnetbase.com/articles/12_21_86.pdf.* (22.12.2020)